Febuxostat inhibits TGF-β1-induced epithelial-mesenchymal transition via downregulation of USAG-1 expression in Madin-Darby canine kidney cells *in vitro*

LINGHONG LU[1*], JIAJUN ZHU[2*], YAQIAN ZHANG[1], YANXIA WANG[1], SHU ZHANG[1] and ANZHOU XIA[1]

[1]Department of Pharmacology, Jiangsu Key Laboratory of New Drug Research and Clinical Pharmacy, Xuzhou Medical University, Xuzhou, Jiangsu 221004; [2]Department of Anesthesiology, Guanyun County People's Hospital, Lianyungang, Jiangsu 222200, P.R. China

Received October 25, 2018; Accepted December 4, 2018

DOI: 10.3892/mmr.2019.9806

Abstract. Our previous study demonstrated that febuxostat, a xanthine oxidase inhibitor, can alleviate kidney dysfunction and ameliorate renal tubulointerstitial fibrosis in a rat unilateral ureteral obstruction (UUO) model; however, the underlying mechanisms remain unknown. Increasing evidence has revealed that epithelial-mesenchymal transition (EMT) is one of the key mechanisms mediating the progression of renal tubulointerstitial fibrosis in chronic kidney disease (CKD). Uterine sensitization-associated gene-1 (USAG-1), a kidney-specific bone morphogenetic protein antagonist, is involved in the development of numerous types of CKDs. The present study aimed to investigate the role of febuxostat in the process of EMT in Madin-Darby canine kidney (MDCK) cells *in vitro*. Western blotting, reverse transcription-semiquantitative polymerase chain reaction analysis and immunofluorescence staining were used to evaluate the expression levels of bone morphogenetic protein 7, USAG-1, α-smooth muscle actin (α-SMA) and E-cadherin, respectively. The results demonstrated that the expression of USAG-1 and α-SMA increased, and that of E-cadherin decreased significantly in MDCK cells following treatment with transforming growth factor-β1 (TGF-β1). The application of small interfering RNA-USAG-1 potently inhibited TGF-β1-induced EMT. Subsequently, the effects of febuxostat on TGF-β1-induced EMT was investigated. The results demonstrated that febuxostat downregulated the expression of USAG-1, and reversed TGF-β1-induced EMT in MDCK cells. Furthermore, pretreatment with febuxostat significantly restored the decreased expression levels of phosphorylated Smad1/5/8 induced by TGF-β1 in MDCK cells. The results of the present study suggested that USAG-1 may be involved in the EMT process of MDCK cells induced by TGF-β1, and febuxostat inhibited EMT by activating the Smad1/5/8 signaling pathway via downregulating the expression of USAG-1 in MDCK cells.

Correspondence to: Professor Anzhou Xia, Department of Pharmacology, Jiangsu Key Laboratory of New Drug Research and Clinical Pharmacy, Xuzhou Medical University, 209 Tongshan Road, Xuzhou, Jiangsu 221004, P.R. China
E-mail: xiaanzhou@xzhmu.edu.cn

*Contributed equally

Key words: febuxostat, epithelial-mesenchymal transition, renal interstitial fibrosis, USAG-1, small interfering RNA-USAG-1

Introduction

Renal interstitial fibrosis, characterized by the activation of interstitial fibroblasts, accumulation of excess extracellular matrix components and tubular atrophy, is a common pathology associated with the progression of chronic kidney disease (CKD) to end-stage renal disease caused by various etiologies (1-3). The aforementioned interstitial and tubular alterations in the progression of CKD may lead to irreversible renal damage and impaired renal function, eventually leading to end-stage renal failure (4,5). Epidemiological studies have demonstrated that the prevalence of CKD is increasing annually worldwide with a high incidence and mortality rate, and has become a major global public health concern (6-8). Therefore, understanding the pathogenesis of the molecular mechanisms underlying tubulointerstitial fibrosis is of great importance to identify novel targets for the effective treatment, prevention and delay of CKD.

Epithelial-mesenchymal transition (EMT) has been reported as the major event characterizing the pathogenesis of renal interstitial fibrosis (9). In the process of EMT, renal tubular epithelial cells lose their unique phenotype and acquire the mesenchymal cell phenotype to differentiate into mesenchymal fibroblasts (10). Increasing evidence has indicated that transforming growth factor- β1 (TGF-β1) is the key factor in the regulation of renal interstitial fibrosis (11-13), and is the most potent inducer in initiating and completing the entire EMT course.

Bone morphogenetic protein-7 (BMP-7) is a homodimeric protein that belongs to the TGF-β superfamily, and has a wide range of biological activities including

the regulation of cell proliferation, and osteogenic and anti-inflammatory activity (14,15). Previous studies have revealed that BMP-7-knockout mice succumbed to mortality shortly after birth due to diffuse renal dysplasia, revealing that BMP-7 is indispensable for normal kidney development (16,17). It has also been reported that the expression of BMP-7 in the kidney is downregulated and gradually becomes more serious with disease progression in the pathogenesis of ischemia-reperfusion injury (18), diabetic nephropathy (19), hypertensive nephrosclerosis (20) and unilateral ureteral obstruction (UUO) (21). In addition, numerous studies have demonstrated that exogenous BMP-7 could inhibit or reverse TGF-β1-induced EMT *in vitro*, prevent or delay the development of fibrosis, and improve renal function in a variety of kidney disease models (22-24); however, the exact molecular mechanism of BMP-7 in improving renal interstitial fibrosis has not been fully elucidated.

Uterine sensitization-associated gene-1 (USAG-1) is a specific antagonist of BMP-7 and is mainly expressed in distal convoluted renal tubular epithelial cells (25). In adult kidneys, it has been reported that USAG-1 is the major negative regulator of BMP function, and binds to BMP-7, thereby inhibiting the interaction between BMP-7 and its receptor, ultimately weakening the renal protective effects of BMP-7 (26). Mice with USAG-1 knockout could promote the expansion of mesenchymal stem cells and accelerate fracture healing, and inhibit the development of renal interstitial fibrosis (27,28). Tanaka *et al* (29) revealed that USAG-1 gene-deficient mice with Alport syndrome had mild renal disease and delayed disease progression. It has been reported that USAG-1 gene defects were more capable of promoting acute kidney injury caused by cisplatin and chronic kidney injury compared with in wild-type mice, while renal protection was suppressed when BMP-7 neutralizing antibodies were administered. Thus, USAG-1 may affect the protective properties of endogenous BMP-7 in the kidney (25,30); however, whether USAG-1 affects the process of renal interstitial fibrosis by altering the occurrence of EMT remains unclear.

Febuxostat, a novel non-selective xanthine oxidase inhibitor, potently reduces uric acid synthesis in the body, decreasing the concentration (31). Febuxostat is mainly used for the treatment of gout in clinical practice (32,33). A recent study demonstrated that febuxostat can also reduce serum uric acid levels, delay the progression of renal dysfunction in patients with chronic kidney disease and reduce the risk of cardiovascular disease, in addition to the treatment of gout (34). It was reported that febuxostat exhibited renal protective effects on cisplatin-induced acute and chronic kidney injury, and streptozotocin-induced diabetic rats in the experimental animal model, and thus could reduce renal tissue damage (35,36). Our previous study also revealed that febuxostat could ameliorate renal interstitial fibrosis caused by UUO (37).

Based on previous studies, the present study aimed to investigate the following: i) The role of USAG-1 in TGF-β1-induced EMT in Madin-Darby canine kidney (MDCK) cells; and ii) whether febuxostat could exert its inhibitory effect on EMT, and if so, whether this inhibitory effect was associated with the downregulation of USAG-1 expression, thereby activating the BMP-7/Smad1/5/8 signaling pathway.

Materials and methods

Cell lines. MDCK cells from Otwo Biotech (Shenzhen) Inc., Guangzhou, China were cultured in RPMI-1640 medium (Gibco; Thermo Fisher Scientific, Inc., Waltham, MA, USA), supplemented with 10% fetal bovine serum (FBS; Hangzhou Sijiqing Bioengineering Material Co., Ltd. Hangzhou, China) and cultured in a 5% CO_2 incubator at 37˚C until 60-70% confluence was attained. Cells were treated with 10 ng/ml human recombinant TGF-β1 (PeproTech, Inc., Rocky Hill, NJ, USA) for 48 h at 37˚C to induce EMT. For experimental use, MDCK cells were treated with RPMI-1640 medium at 37˚C, containing 1% FBS (Hangzhou Sijiqing Bioengineering Material Co., Ltd.) for 12 h, and then treated with 10 ng/ml TGF-β1 combined with or without low (0.1 μM), middle (1 μM) or high (10 μM) concentrations of febuxostat for 48 h at 37˚C. All experiments were performed three times. Following treatment for 48 h, the cells were harvested for detection.

MTT assay for cell viability analysis. MDCK cells were seeded into 96-well culture plates and incubated with 1% FBS for 12 h when the cells were attached, followed by treatment with different concentrations of febuxostat for 48 h. Cell viability was determined using an MTT assay. Subsequently, cells were incubated with MTT solution (0.5 mg/ml) for 4 h at 37˚C. The purple formazan crystals derived from the addition of MTT were dissolved in dimethyl sulfoxide and agitated for 10 min. The absorbance at 490 nm was measured using a microplate reader (BioTek Instruments, Inc., Winooski, VT, USA).

RNA interference. The sequences of small interfering (si)RNA-control (si-ctrl) and siRNA-USAG-1 interference plasmids flanked by EcoRI and AgeI restriction site were constructed into the H1 promoter of lentivirus infectious virions pGLV3-H1-GFP-Puro (Public Protein/Plasmid Library Biotechnology Co., Ltd. Nanjing, China). The negative control siRNA was designed as: Forward, 5'-TTC TCCGAACGTGTCACGTAA-3'; the siRNA-USAG-1 was designed as: Forward, 5'-CCTCCTGCCATTCATTTC TT-3'. Cells ($1.0x10^6$/ml) were plated into 6-mm wide petri dish and cultured in RPMI-1640 medium. A total of 5 μg siRNA-expressing plasmids and 10 μl Lipofectamine® 2000 (Thermo Fisher Scientific, Inc.) were used for transfection when cell confluency reached 70-80%. MDCK cells were divided into the blank group, si-ctrl, TGF-β1 (10 ng/ml) stimulation (TGF-β1), TGF-β1 (10 ng/ml) plus siRNA-control (TGF-β1 + si-ctrl), and TGF-β1 (10 ng/ml) plus siRNA-USAG-1 group (TGF-β1 + si-USAG-1). Following transfection for 6 h, the medium was removed and cells were cultured in serum-free medium containing 10% FBS without antibiotics. Following transfection for 22 h, the cells were treated with 10 ng/ml TGF-β1, containing 1% FBS for 48 h at 37˚C, and after 70 h of transfection, the cells were collected for experimentation.

RNA isolation and reverse transcription (RT-) semi-quantitative polymerase chain reaction (sqPCR)

analysis. Total RNA was extracted from MDCK cells using TRIzol® reagent (Invitrogen; Thermo Fisher Scientific, Inc.), according to manufacturer's protocols. RT of total RNA was performed using the TIANScript RT kit (Tiangen Biotech Co., Ltd., Beijing, China) with the following temperature protocol: 42˚C for 50 min, 95˚C for 5 min, then held at 4˚C. The primers of α-smooth muscle actin (α-SMA) and E-cadherin were synthesized by Sangon Biotech Co., Ltd. (Shanghai, China). The primer sequences were as follows: α-SMA forward, 5'-GTGATGGTGGGGATGGGACAA-3' and reverse, 5'-CCAGAGGCGTAGAGGGAAAGC-3' (311 bp); E-cadherin forward, 5'-CAGCATCCTCACACA AGACC-3' and reverse, 5'-TCAGCATCCGTCACTTTG AG-3' (300 bp); GAPDH forward, 5'-CTTGAAAGGCGG GGCCAAGAGG-3' and reverse, 5'-ACTGATACATTGGGG GTGGGGACA-3' (393 bp). sqPCR was performed using the 2XTaq PCR MasterMix (Tiangen Biotech Co., Ltd. Beijing, China) with initial denaturation at 94˚C for 5 min, followed by 30 consecutive cycles of denaturation at 94˚C for 30 sec, annealing at 58-62˚C for 30 sec, extension at 72˚C for 1 min, and then a final extension at 72˚C for 7 min using a thermal cycler system (Applied Biosystems; Thermo Fisher Scientific, Inc.). The amplified products were analyzed by electrophoresis on a 1.5% (w/v) agarose gel which was stained with fluorescence staining dye Goldview (Beijing Solarbio Science and Technology Co., Ltd. Beijing, China) at 60˚C. The gel was congealed at room temperature for 30 min. The electrophoresis continued for 50 min at 110 V. The relative abundance of mRNAs was measured using GAPDH mRNA expression levels as the internal reference. The signal intensity of the images was analyzed using ImageJ version 1.48 software (National Institutes of Health, Bethesda, MD, USA).

Western blot analysis. Proteins were extracted from MDCK cells using radioimmunoprecipitation assay lysis buffer containing RIPA and the protease inhibitor PMSF (both Beyotime Institute of Biotechnology, Shanghai, China). The compounds were placed at 4˚C for at least 60 min and then centrifuged at 4˚C and 10,000 x g for 15 min. The supernatant was collected for western blotting. Protein concentration in the supernatant was determined using the BCA protein assay kit (Beyotime Institute of Biotechnology). Equal amounts of protein (60 μg) were separated using SDS-PAGE (8-10%) and transferred onto nitrocellulose membranes. The membranes were then blocked in PBS containing 3% bovine serum albumin (BSA; Vicmed Biotech Co. Ltd., Xuzhou, China) and incubated with primary antibodies, including anti-E-cadherin (1:1,000; cat. no. ab1416), anti-α-SMA (1:1,000; cat. no. ab7817), anti-USAG-1 (1:1,000; cat. no. ab99340; all Abcam, Cambridge, UK), anti-p-Smad1/5/8 (1:1,000; cat. no. 13820; Cell Signaling Technology, Inc., Danvers, MA, USA) and anti-Smad1/5/8 (1:1,000; cat. no. sc-6031-R; Santa Cruz Biotechnology, Inc., Dallas, TX, USA) overnight at 4˚C. Near-infrared fluorescence-conjugated goat anti-rabbit (1:1,000; cat. no. V926-32211) or anti-mouse (1:1,000; cat. no. V926-32210; both Vicmed Biotech Co. Ltd.) secondary antibodies were used to incubate the membranes for 1 h at room temperature, which were developed colorimetrically via the Odyssey biocolor infrared fluorescence imaging system (LI-COR Biosciences, Lincoln, NE, USA). Quantification was performed by measuring the intensity of the signals using ImageJ software version 1.48 by quantifying the relative expression of target protein vs. GAPDH.

Immunofluorescence staining analysis. MDCK cells ($1.0x10^4$/ml) were seeded into 12-well plates with pre-placed slides. Following the adherence of cells, the cells were allowed to stand for 12 h with 1% FBS, prior to being washed with PBS twice and treated with TGF-β1 with or without different concentrations of febuxostat (0.1, 1 or 10 μM) for 48 h. After 48 h, the cells were washed with PBS for three times for 5 min per wash and fixed at room temperature for 30 min with 4% paraformaldehyde; 0.5% TritonX-100 was added to permeabilize cells for 10 min. Cells were subsequently washed with PBS three times for 5 min each time and covered with 2% BSA (Vicmed Biotech Co. Ltd.) for 30 min at 37˚C. Next, cells were incubated with USAG-1 (1:200; cat. no. ab99340), α-SMA (1:200; cat. no. ab7817; both Abcam) or E-cadherin (1:200; cat. no. 14472; Cell Signaling Technology, Inc.) antibodies, which had been diluted in PBS overnight at 4˚C. Subsequently, the cells were incubated with goat anti-rabbit (1:500; cat. no. A-11034; Alexa Fluor 488) or anti-mouse (1:500; cat. no. A-11004; Alexa Fluor 568; both Thermo Fisher Scientific, Inc.) secondary antibodies for 2 h at 37˚C and were then stained with the nuclear-specific stain DAPI (Beyotime Institute of Biotechnology) for 3 min at room temperature. Following three washes with PBS for 5 min per wash, anti-fluorescence quenching liquid (Beyotime Institute of Biotechnology) was added to the clean glass slides and cells were analyzed under an Olympus BX43F fluorescence microscope (Olympus Corporation, Tokyo, Japan). The excitation light of goat anti-rabbit secondary antibody is 488 nm, and the excitation light of goat anti-mouse secondary antibody is 568 nm. Digital images were captured using an inverted fluorescent microscope (magnification, x400).

Statistical analysis. Data are presented as the mean ± standard error of the mean. Statistical analysis was performed using SPSS 16.0 statistical software (SPSS, Inc., Chicago, IL, USA). Comparison between groups was conducted using one-way analysis of variance, followed by the Least Significant Difference test with homogeneity of variances, or the Dunnett's T3 test with heterogeneity of variances. $P<0.05$ was considered to indicate a statistically significant difference. All experiments were performed three times.

Results

TGF-β1 upregulates the expression of USAG-1 and induces EMT in MDCK cells, whereas USAG-1 gene silencing prevents TGF-β1-induced EMT. According to the western blotting results, transfection with siRNA-USAG-1 significantly decreased the protein expression of USAG-1 compared with the siRNA-control group (Fig. 1A). Following treatment with TGF-β1, the protein expression levels of USAG-1 (Fig. 1B) and α-SMA (Fig. 1C) were significantly increased, while that of E-cadherin (Fig. 1D) was significantly decreased in MDCK cells compared with the blank group ($P<0.01$). Additionally, it was also demonstrated

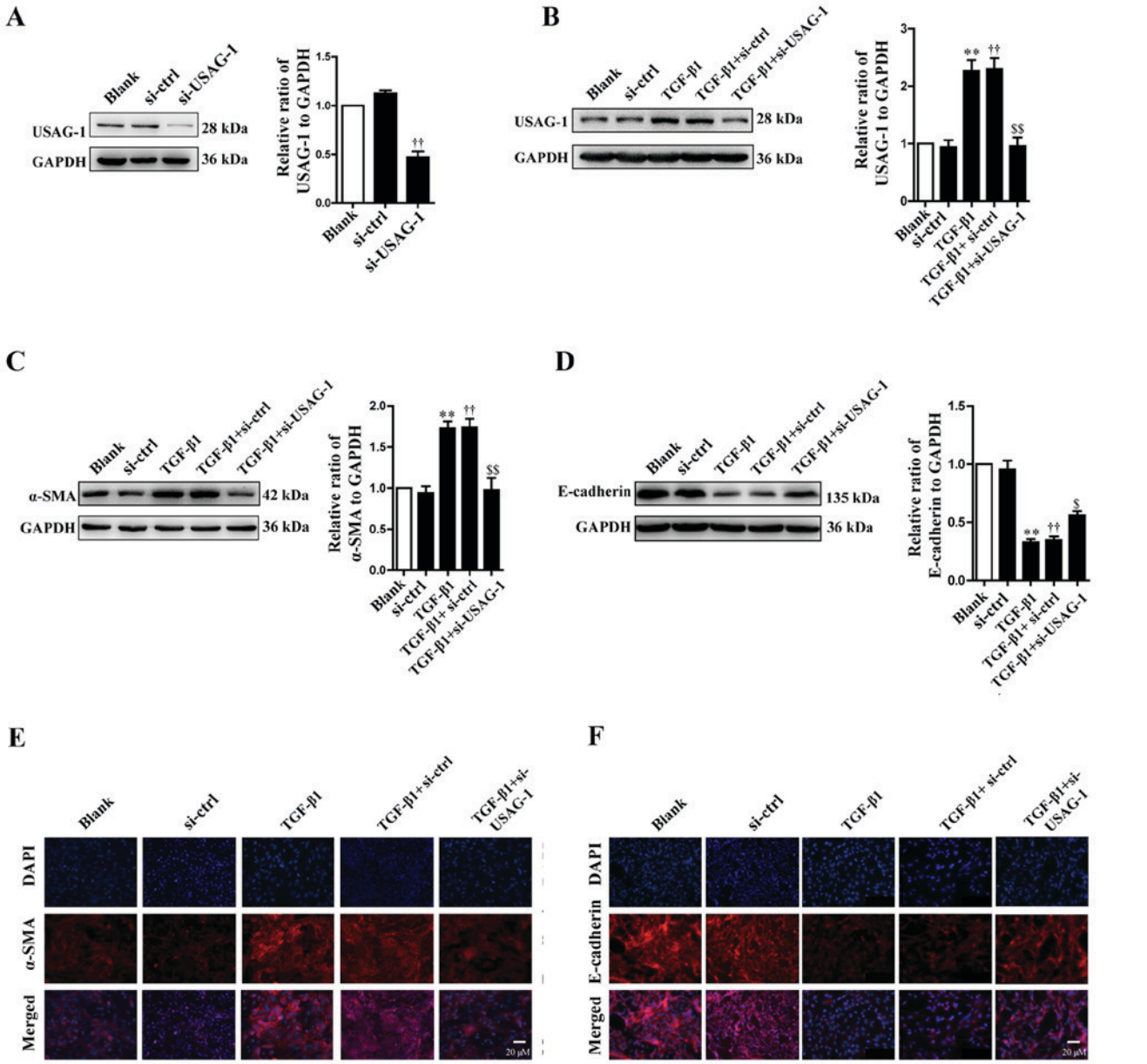

Figure 1. Effects of USAG-1 on epithelial-mesenchymal transition induced by TGF-β1 in MDCK cells. MDCK cells were transfected with a negative control siRNA or a siRNA-USAG-1 plasmid for 70 h. The protein expression levels of (A and B) USAG-1, (C) α-SMA and (D) E-cadherin were evaluated using western blotting. All the data are presented as the mean ± standard error of the mean, n=3. **P<0.01 vs. blank group; ††P<0.01 vs. siRNA-ctrl; $^{\$}$P<0.05 and $^{\$\$}$P<0.01 vs. TGF-β1 + siRNA-ctrl group. Immunofluorescence staining demonstrated the labeling intensity of (E) α-SMA (red staining) and (F) E-cadherin (red staining). Magnification, x400. α-SMA, α-smooth muscle actin; MDCK, Madin-Darby canine kidney; si, small interfering RNA; si-ctrl, siRNA-control; si-USAG-1, siRNA-USAG-1; TGF-β1, transforming growth factor-β1; USAG-1, uterine sensitization-associated gene-1.

that transfection with USAG-1-specific siRNA for 70 h and TGF-β1 treatment significantly decreased the protein expression of α-SMA (Fig. 1C), while that of E-cadherin was increased compared with the TGF-β1 + siRNA-control group (P<0.01; Fig. 1D). Immunofluorescence revealed that the findings were consistent with those of western blotting. MDCK cells treatment with TGF-β1 exhibited an increased intensity of anti-α-SMA labeling (Fig. 1E, red staining) and a decreased intensity of anti-E-cadherin labeling (Fig. 1F, red staining); however, siRNA-USAG-1 reversed the these alterations induced by TGF-β1 (Fig. 1E and F). Notable differences were observed in protein expression between the blank and the siRNA-control groups, or the TGF-β1 and TGF-β1 + siRNA-control groups. Collectively, these findings indicated that USAG-1 may promote the occurrence of EMT induced by TGF-β1 in MDCK cells.

USAG-1 inhibits the activity of the Smad1/5/8 signaling pathway in TGF-β1-induced EMT. USAG-1 is a specific antagonist of BMP-7, and Smad1/5/8 are the key intracellular signaling proteins of BMP-7; the phosphorylation of Smad1/5/8 is a central downstream element of BMP signal transduction (30,38). Therefore, the present study examined the levels of phosphorylated and total Smad1/5/8 by western blot analysis. Compared with the blank group, the phosphorylation levels of Smad1/5/8 were significantly decreased in MDCK cells following treatment with TGF-β1; the phosphorylation levels of Smad1/5/8 were significantly

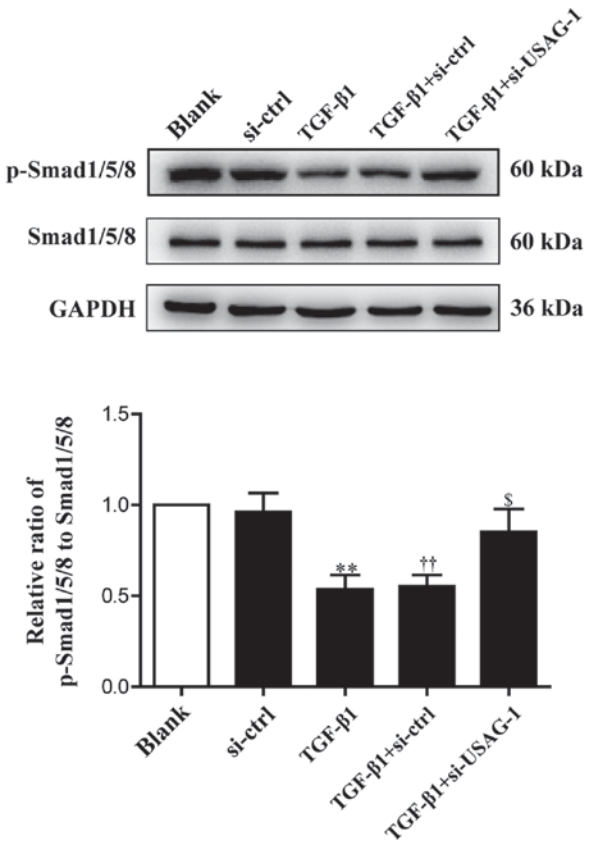

Figure 2. Effects of USAG-1 silencing on the expression of p-Smad1/5/8. Madin-Darby canine kidney cells were transfected with a negative control siRNA or a siRNA-USAG-1 plasmid for 70 h. The expression levels of p-Smad1/5/8 were evaluated using western blotting. All the data are presented as the mean ± standard error of the mean, n=3. **P<0.01 vs. blank group; ††P<0.01 vs. siRNA-ctrl; $^{\$}$P<0.05 vs. TGF-β1 + siRNA-ctrl group. p, phosphorylated; si, small interfering RNA; si-ctrl, siRNA-control; si-USAG-1, siRNA-USAG-1; TGF-β1, transforming growth factor-β1; USAG-1, uterine sensitization-associated gene-1.

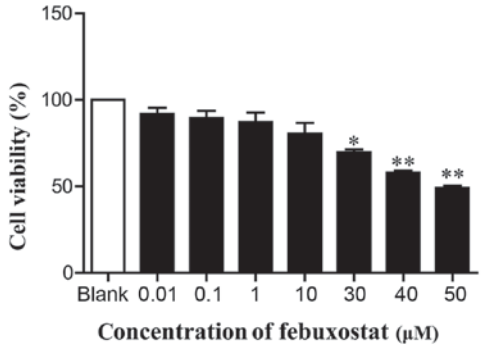

Figure 3. Effects of febuxostat on the viability of MDCK cells. MDCK cells were incubated with different concentrations of febuxostat (0.01, 0.1, 1, 10, 30, 40 and 50 μM) for 48 h; 0 μM febuxostat was represented as the blank group. All the data are presented as the mean ± standard error of the mean, n=3. *P<0.05, **P<0.01 vs. blank group. MDCK, Madin-Darby canine kidney.

upregulated compared with the TGF-β1 + siRNA-control group, almost to basal levels of the blank group following si-USAG-1 transfection and TGF-β1 treatment (Fig. 2). No significant difference was observed in the protein expression levels between the blank and the siRNA-control groups, or the TGF-β1 and TGF-β1 + siRNA-control groups. These results indicated that USAG-1 may promote the occurrence of EMT by, at least partly, inhibiting the activity of the Smad1/5/8 signaling pathway.

Effects of febuxostat on cell viability. In order to examine the effects of febuxostat on the viability of MDCK cells, cells were treated with various concentrations of febuxostat for 48 h. The results revealed that concentrations of febuxostat at 30, 40 and 50 μM significantly reduced cell viability compared with the blank group. Conversely, there was no or little effects on cell viability at doses of 0.01, 0.1, 1 and 10 μM febuxostat compared with the blank group (Fig. 3). Considering the effects of febuxostat on cell viability and the results of MTT assay, concentrations of 0.1, 1 and 10 μM febuxostat were selected for subsequent experiments.

Febuxostat inhibits the expression of USAG-1 in MDCK cells. The expression of USAG-1 in MDCK cells was detected by western blotting and immunofluorescence staining. Immunoblotting demonstrated that middle and high concentrations of febuxostat significantly decreased the expression of USAG-1, while a low concentration had no significant effect on expression compared with the TGF-β1 group (Fig. 4A). Immunofluorescence staining further revealed that the labeling intensity of USAG-1 (red staining) notably increased following TGF-β1 treatment; however, low, middle and high concentrations of febuxostat weakened the increased labeling intensity of USAG-1 induced by TGF-β1, particularly when middle and high concentrations of febuxostat were applied (Fig. 4B).

Febuxostat inhibits the EMT of MDCK cells induced by TGF-β1. EMT is an important mechanism that induces renal interstitial fibrosis, and it is essential for the development of chronic kidney disease (39). To investigate the role of febuxostat in TGF-β1-induced EMT, the expression levels of the epithelial marker, E-cadherin, and the mesenchymal marker, α-SMA, were determined by semi-qPCR and western blotting. MDCK cells exposed to TGF-β1 for up to 48 h exhibited a significant increase in α-SMA at the mRNA (Fig. 5A) and protein (Fig. 5B) expression levels (P<0.01), while the expression levels of E-cadherin at the mRNA (Fig. 5C) and protein (Fig. 5D) expression levels were significantly decreased, compared with in the blank group (P<0.01). Conversely, middle and high concentrations of febuxostat significantly reversed the downregulation of E-cadherin mRNA and protein expression (Fig. 5C and D) stimulated by TGF-β1; a low concentration of febuxostat significantly affected the mRNA expression of E-cadherin compared with TGF-β1 treatment alone (Fig. 5C). In addition, there were no notable effects on the expression of α-SMA at the mRNA and protein expression levels following treatment with a high concentration of febuxostat in normal cells.

The fluorescence intensity of USAG-1 (green staining) co-stained with α-SMA (red staining) or E-cadherin (red staining) was further investigated by double immunofluorescence staining (Fig. 6). MDCK cells treated with TGF-β1 exhibited a strong fluorescence intensity for USAG-1 and α-SMA, but the fluorescence intensity for E-cadherin was weak compared with the blank group. Treatment with febuxostat reversed these effects. Furthermore, double immunolabeling

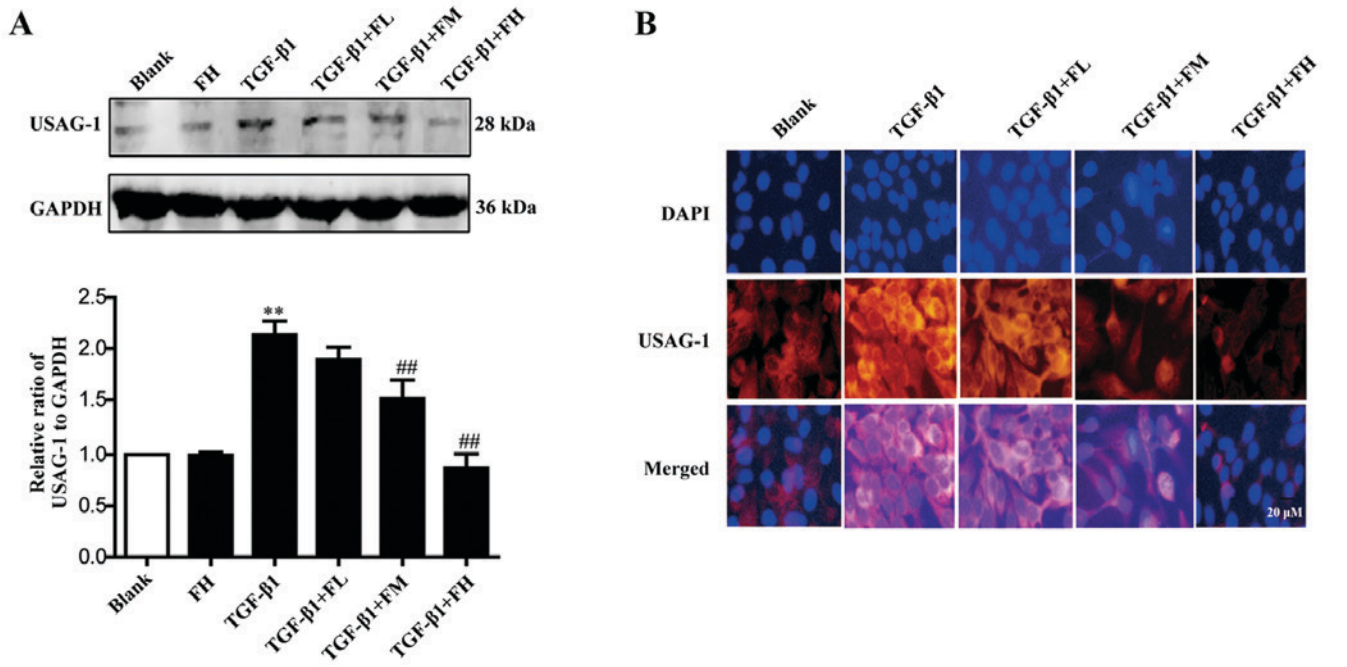

Figure 4. Effects of febuxostat on the expression of USAG-1 protein in TGF-β1-treated Madin-Darby canine kidney cells. Cells were incubated with different concentrations of febuxostat with or without TGF-β1 for 48 h. The protein expression of USAG-1 was evaluated by (A) western blotting and (B) immunofluorescence staining. There were no significant effects on the protein expression of USAG-1 when cells were treated with a high concentration of febuxostat in normal cells. All the data are presented as the mean ± standard error of the mean, n=3. **P<0.01 vs. blank group; $^{\#\#}$P<0.01 vs. TGF-β1 group. USAG-1, uterine sensitization-associated gene-1.

indicated that USAG-1 co-expressed with α-SMA (Fig. 6A) or E-cadherin (Fig. 6B) in the same MDCK cells; the notably increased labeling intensity of USAG-1 in MDCK cells tended to be accompanied by strong α-SMA labeling intensity or a weak labeling of E-cadherin, and vice versa.

The aforementioned results suggested that febuxostat could reverse the occurrence of EMT in MDCK cells induced by TGF-β1; the underlying mechanism may be at least partly associated with the downregulation of USAG-1.

Effects of febuxostat on the activity of the Smad1/5/8 signaling pathway in MDCK cells. To determine the effect of febuxostat on the activity of the Smad1/5/8 signaling pathway, the levels of p-Smad1/5/8 and total Smad1/5/8 in MDCK cells were examined. Western blotting demonstrated that TGF-β1 significantly decreased the expression levels of p-Smad1/5/8, indicating a reduced activity of Smad1/5/8 signaling. Compared with the TGF-β1 group, treatment with different concentrations of febuxostat significantly increased the levels of p-Smad1/5/8. Febuxostat alone had no significant effect on the expression of p-Smad1/5/8 in uninduced cells. These results suggested that the Smad1/5/8 signaling pathway is involved in the TGF-β1-induced EMT process, and these effects may be inhibited by febuxostat (Fig. 7).

Discussion

Our previous study reported that febuxostat was able to ameliorate renal tubulointerstitial fibrosis in a rat model of UUO (37). The present study reported that USAG-1 served an important role in the onset of TGF-β1-induced EMT, and that febuxostat exerts its inhibitory effect on EMT by inhibiting the expression of USAG-1 and activating the Smad1/5/8 signaling pathway.

Renal interstitial fibrosis is the final outcome of the development of all types of CKD, and is associated with the progression of chronic renal failure, the main cause of end-stage renal failure (3). Recent studies have demonstrated that almost all types of renal injury can induce the occurrence of EMT in renal tubular epithelial cells, which is an important process in the pathogenesis of tubulointerstitial fibrosis (39,40). EMT is characterized by the loss of epithelial cell characteristics and the acquisition of mesenchymal markers due to excessive exposure to a variety of profibrotic cytokines (2). TGF-β1 is a well-characterized fibrogenic cytokine, which is associated with renal diseases and serves a key role in EMT (11). The present study revealed that TGF-β1 could induce EMT in MDCK cells. Following 48 h of TGF-β1 treatment, EMT was readily induced in MDCK cells, as determined by the downregulation of E-cadherin for the epithelial phenotype, and upregulation of α-SMA for the mesenchymal phenotype. These results demonstrated that TGF-β1 is capable of successfully inducing EMT, which is consistent with a previous report (41).

BMP-7, formerly known as osteogenic protein-1, is a member of the BMP-subfamily within the TGF-β superfamily, and serves an important role in maintaining the function of renal tubular epithelial cells (42). It has been reported that BMP-7 could upregulate the expression of E-cadherin in human fibroblasts induced by TGF-β1, and reduce the secretion of proinflammatory cytokines and growth factors, inhibiting or reversing the renal tubular EMT process; thus, the formation of renal fibrosis is reduced (43). The Smad signaling pathway is essential for TGF-β1-induced EMT. Increasing

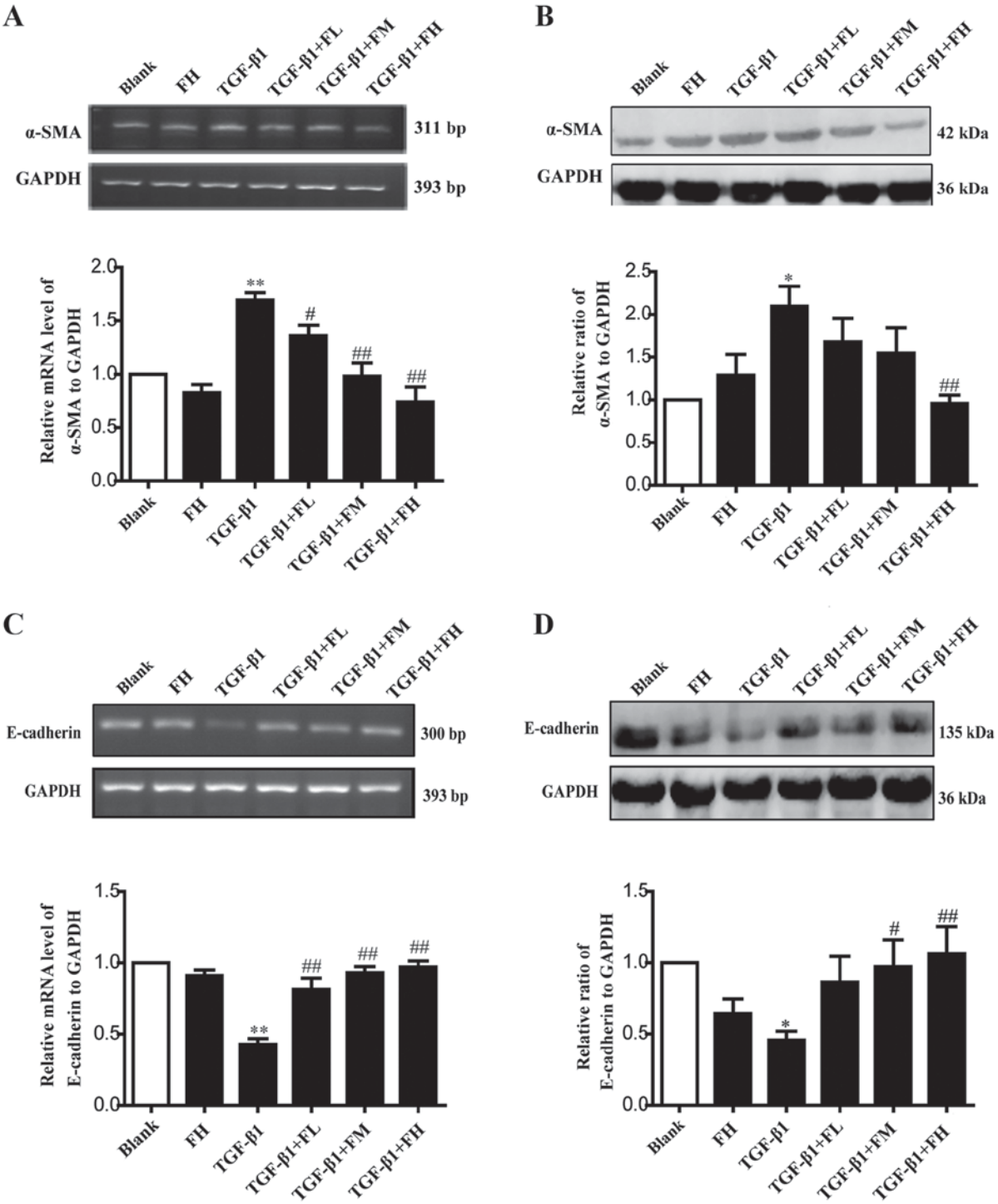

Figure 5. Effects of febuxostat on the expression of α-SMA and E-cadherin at the mRNA and protein levels in MDCK cells. Incubation of MDCK cells with various concentrations of febuxostat in the presence or absence of TGF-β1 for 48 h. (A) mRNA and (B) protein expression levels of α-SMA were determined by semi-qPCR and western blotting, respectively. (C) mRNA and (D) protein expression levels of E-cadherin were determined by semi-qPCR and western blotting, respectively. All the data are presented as the mean ± standard error of the mean, n=3. *P<0.05 and **P<0.01 vs. blank group; $^{\#}$P<0.05 and $^{\#\#}$P<0.01 vs. TGF-β1 group. α-SMA, α-smooth muscle actin; FH, high-concentration febuxostat; FL, low-concentration febuxostat; FM, middle-concentration febuxostat; MDCK, Madin-Darby canine kidney; qPCR, quantitative polymerase chain reaction; TGF-β1, transforming growth factor-β1.

evidence has indicated that BMP-7 could inhibit or reverse renal interstitial fibrosis in animal models by regulating downstream of the Smad1/5/8 signaling pathway (19,21,38). BMP-7 activity in the kidney is not only determined by the availability of BMP-7 itself, but also by the balance of antagonists (44). USAG-1, a specific BMP-7 antagonist that is mainly produced by renal distal tubular epithelial cells of the adult kidney, serves a critical role in the modulation of the renoprotective action of BMP-7 (45). Therefore, the present study investigated the effects of USAG-1 on TGF-β1-induced EMT and the activity of the p-Smad1/5/8 pathway in MDCK cells by dysregulating the expression of USAG-1. The results of the present study demonstrated that TGF-β1 upregulated the expression of USAG-1 and α-SMA, but downregulated

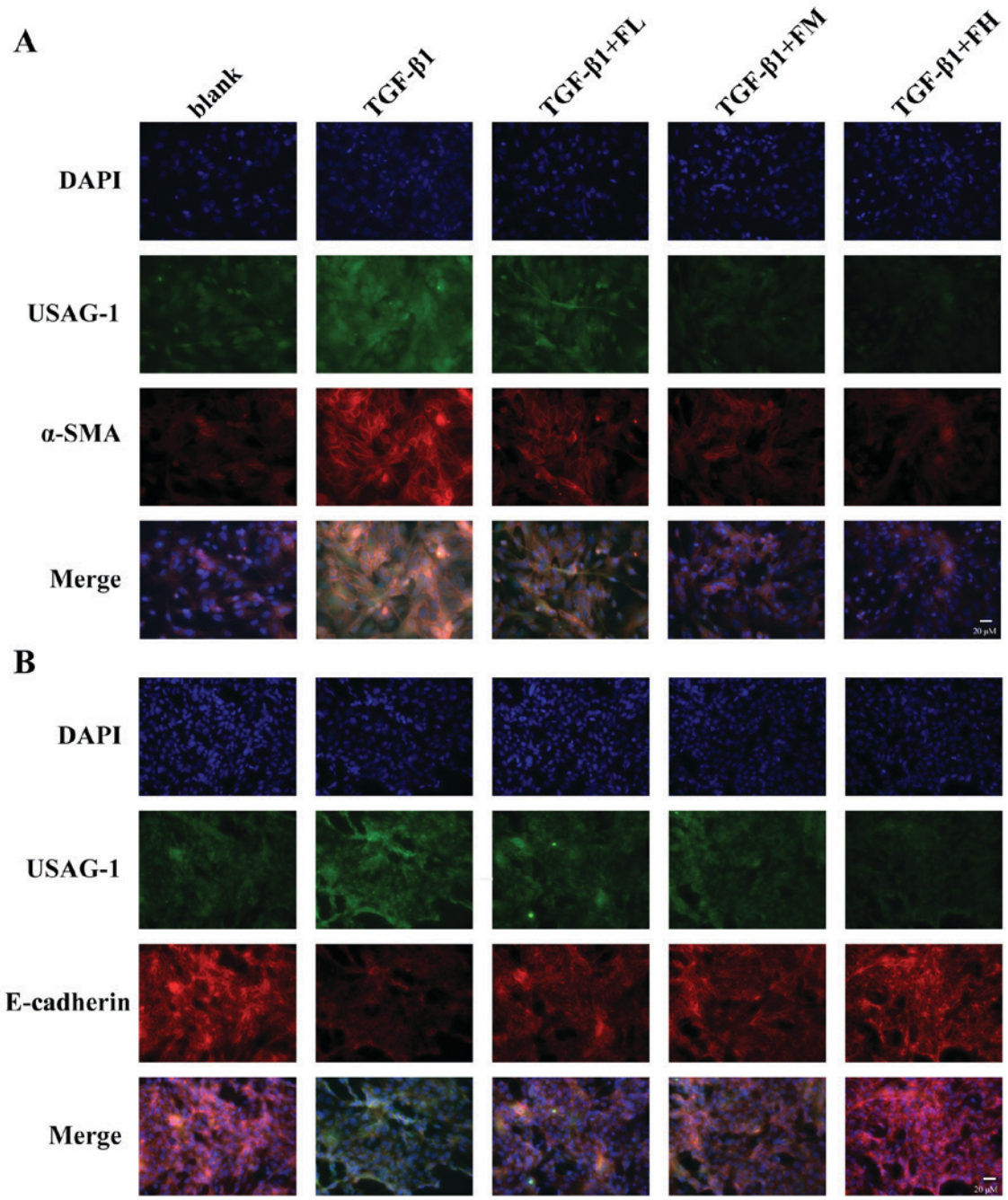

Figure 6. Double immunofluorescence for (A) α-SMA/USAG-1 and (B) E-cadherin/USAG-1 in TGF-β1-induced MDCK cells. Incubation of MDCK cells with different concentrations of febuxostat in the presence or absence of TGF-β1 for 48 h. USAG-1 was identified as green staining, α-SMA and E-cadherin were identified as red staining. Magnification, x400. α-SMA, α-smooth muscle actin; FL, low-concentration febuxostat; FM, moderate-concentration febuxostat; FH, high-concentration febuxostat; MDCK, Madin-Darby canine kidney; TGF-β1, transforming growth factor-β1; USAG-1, uterine sensitization-associated gene-1.

that of E-cadherin and p-Smad1/5/8 protein, which were statistically significantly different to the expression profiles in the control group. Conversely, siRNA-USAG-1 significantly decreased the expression of α-SMA, and increased the protein expression levels of E-cadherin and p-Smad1/5/8. Therefore, it may be suggested that USAG-1 is involved in promoting the occurrence of EMT in MDCK cells, and its mechanism may be associated with downregulation of the activity of the Smad1/5/8 signaling pathway.

Due to the important role of EMT in renal fibrosis, any therapeutic strategy that targets the EMT may improve fibrosis. Febuxostat, a xanthine oxidase inhibitor, achieves its therapeutic effect by decreasing the levels of uric acid in the serum (31). The results of early animal experiments indicated that febuxostat could alleviate kidney dysfunction in patients, and improve renal interstitial fibrosis in a rat model of UUO (37,46); however, whether febuxostat serves a role in preventing renal tubular EMT induced by TGF-β1 remains unknown. In the present study, it was observed that the protein expression levels of USAG-1 were significantly increased in the TGF-β1 group; however, febuxostat treatment suppressed the expression of USAG-1 and α-SMA, while upregulating

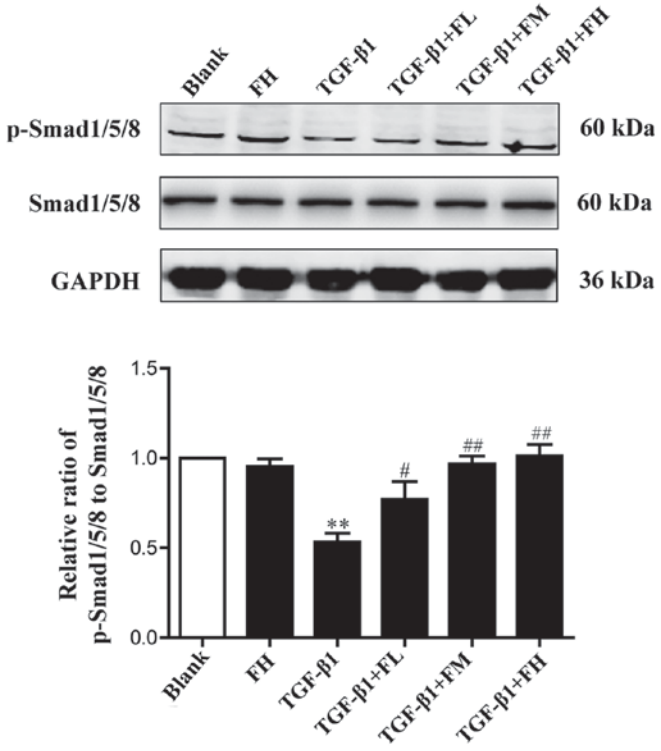

Figure 7. Effects of febuxostat on the protein expression of p-Smad1/5/8 in TGF-β1-induced MDCK cells. Incubation of MDCK cells with different concentrations of febuxostat in the presence or absence of TGF-β1 for 48 h. All the data are presented as the mean ± standard error of the mean, n=3. **P<0.01 vs. blank group; $^{\#}$P<0.05 and $^{\#\#}$P<0.01 vs. TGF-β1 group. FL, low-concentration febuxostat; FM, moderate-concentration febuxostat; FH, high-concentration febuxostat; MDCK, Madin-Darby canine kidney; p, phosphorylated; TGF-β1, transforming growth factor-β1.

that of E-cadherin, suggesting that the anti-EMT effect of febuxostat may be associated with the downregulation of USAG-1 expression in MDCK cells.

BMP-7 serves a key role in the phosphorylation of Smad1/5/8 in the transcription of target genes. It has been revealed that the BMP-7-Smad1/5/8 signaling pathway was suppressed in a UUO rat model (37). The signaling pathway is activated while kidney obstruction is repaired, suggesting that the BMP-7-Smad1/5/8 signaling pathway serves an important role in the treatment of renal interstitial fibrosis (38). Therefore, the phosphorylation levels of Smad1/5/8 in TGF-β1-induced EMT in MDCK cells was measured in the present study. The phosphorylation levels of BMP-7 downstream protein Smad1/5/8 appeared to be maintained in normal MDCK cells, but was decreased following treatment with TGF-β1. Nevertheless, the phosphorylation level of Smad1/5/8 protein was significantly increased following the treatment with febuxostat in MDCK cells. Therefore, it is also possible that febuxostat may downregulate the expression of the BMP-7 antagonist USAG-1, which in turn enhances the activity of the Smad1/5/8 signaling pathway, ultimately inhibiting TGF-β1-induced EMT in MDCK cells.

Homeobox protein Hox-A13 (HOXA13), a transcriptional factor encoded by a homeobox gene, can bind to the promoter region of USAG-1 and negatively modulating expression (47). A recent study revealed that albumin could significantly inhibit HOXA13 expression in time- and dose-dependent manners in HKC renal tubular epithelial cells, and the upregulation of HOXA13 could exert a beneficial effect in albumin-induced EMT in HKC cells (48). Additionally, it has been reported that EMT-induced by albumin in HK-2 cells is directly mediated by the production of reactive oxygen species (ROS) (49,50). Therefore, the increased production of ROS may be the leading cause of the reduced HOXA13 expression in albumin-induced EMT. Febuxostat, a non-purine selective xanthine oxidase inhibitor, can effectively inhibit ROS production in various diseases and conditions such as ischemia/reperfusion injury (51,52), atherosclerosis (53). Based the aforementioned reports, decreased ROS production by febuxostat could upregulate the expression of HOXA13 and subsequently inhibit the expression of USAG-1 in MDCK cells, thereby reversing the occurrence of TGF-β1-induced EMT; however, the exact mechanism of action of febuxostat on USAG-1 requires further investigation.

In summary, the results of the present study provided evidence that USAG-1 may be involved in the process of EMT induced by TGF-β1, and febuxostat could reduce the expression of USAG-1 and activate the BMP-7-Smad1/5/8 signaling pathway, thereby reversing the occurrence of EMT. The present study not only provides a theoretical basis for the treatment of renal interstitial fibrosis using febuxostat in clinical practice, but also proposes USAG-1 as a potential therapeutic target in the treatment of kidney disease.

Acknowledgments

Not applicable.

Funding

The present study was funded by a grant from the Director Fund Project of Jiangsu Key Laboratory of New Drug and Clinical Pharmacy, Xuzhou Medical University (grant no. ZR-XY201408).

Availability of data and materials

The datasets used and/or analyzed during the current study are available from the corresponding author on reasonable request.

Authors' contributions

AX, LL and JZ made substantial contributions to the conception and design of the present study. YZ and LL performed the experiments. AX, LL and YZ wrote the manuscript. YW and SZ performed the statistical analysis and edited the manuscript. All authors agree to be accountable for all aspects of the research in ensuring that the accuracy or integrity of any part of the study are appropriately investigated and resolved. All authors read and approved the final version of the manuscript.

Ethics approval and consent to participate

Not applicable.

Patient consent for publication

Not applicable.

Competing interests

The authors declare that they have no competing interests.

References

1. Coca SG, Singanamala S and Parikh CR: Chronic kidney disease after acute kidney injury: A systematic review and meta-analysis. Kidney Int 81: 442-448, 2012.
2. Boor P, Ostendorf T and Floege J: Renal fibrosis: Novel insights into mechanisms and therapeutic targets. Nat Rev Nephrol 6: 643-656, 2010.
3. Becker GJ and Hewitson TD: The role of tubulointerstitial injury in chronic renal failure. Curr Opin Nephrol Hypertens 9: 133-138, 2000.
4. Wynn TA: Common and unique mechanisms regulate fibrosis in various fibroproliferative diseases. J Clin Invest 117: 524-529, 2007.
5. Sulikowska B, Rutkowski B, Marszałek A and Manitius J: The role of interstitial changes in the progression of chronic kidney disease. Postepy Hig Med Dosw (Online) 69: 830-837, 2015.
6. Levin A: Improving global kidney health: International society of nephrology initiatives and the global kidney health atlas. Ann Nutr Metab 72 (Suppl 2): S28-S32, 2018.
7. Jager KJ and Fraser SDS: The ascending rank of chronic kidney disease in the global burden of disease study. Nephrol Dial Transplant 32 (Suppl_2): ii121-ii128, 2017.
8. Jha V, Garcia-Garcia G, Iseki K, Li Z, Naicker S, Plattner B, Saran R, Wang AY and Yang CW: Chronic kidney disease: Global dimension and perspectives. Lancet 382: 260-272, 2013.
9. Sun YB, Qu X, Caruana G and Li J: The origin of renal fibroblasts/myofibroblasts and the signals that trigger fibrosis. Differentiation 92: 102-107, 2016.
10. Cannito S, Novo E, di Bonzo LV, Busletta C, Colombatto S and Parola M: Epithelial-mesenchymal transition: From molecular mechanisms, redox regulation to implications in human health and disease. Antioxid Redox Signal 12: 1383-1430, 2010.
11. Meng XM, Nikolic-Paterson DJ and Lan HY: TGF-β: The master regulator of fibrosis. Nat Rev Nephrol 12: 325-338, 2016.
12. Liu JH, He L, Zou ZM, Ding ZC, Zhang X, Wang H, Zhou P, Xie L, Xing S and Yi CZ: A novel inhibitor of homodimerization targeting MyD88 ameliorates renal interstitial fibrosis by counteracting TGF-β1-induced EMT in vivo and in vitro. Kidney Blood Press Res 43: 1677-1687, 2018.
13. Bae E, Kim SJ, Hong S, Liu F and Ooshima A: Smad3 linker phosphorylation attenuates Smad3 transcriptional activity and TGF-β1/Smad3-induced epithelial-mesenchymal transition in renal epithelial cells. Biochem Biophys Res Commun 427: 593-599, 2012.
14. Bei K, Du Z, Xiong Y, Liao J, Su B and Wu L: BMP7 can promote osteogenic differentiation of human periosteal cells in vitro. Mol Biol Rep 39: 8845-8851, 2012.
15. Singla DK, Singla R and Wang J: BMP-7 treatment increases M2 macrophage differentiation and reduces inflammation and plaque formation in Apo E-/- Mice. PLoS One 11: e0147897, 2016.
16. Dudley AT, Lyons KM and Robertson EJ: A requirement for bone morphogenetic protein-7 during development of the mammalian kidney and eye. Genes Dev 9: 2795-2807, 1995.
17. Luo G, Hofmann C, Bronckers AL, Sohocki M, Bradley A and Karsenty G: BMP-7 is an inducer of nephrogenesis, and is also required for eye development and skeletal patterning. Genes Dev 9: 2808-2820, 1995.
18. Almanzar MM, Frazier KS, Dube PH, Piqueras AI, Jones WK, Charette MF and Paredes AL: Osteogenic protein-1 mRNA expression is selectively modulated after acute ischemic renal injury. J Am Soc Nephrol 9: 1456-1463, 1998.
19. Ivanac-Janković R, Ćorić M, Furić-Čunko V, Lovičić V, Bašić-Jukić N and Kes P: BMP-7 protein expression is down-regulated in human diabetic nephropathy. Acta Clin Croat 54: 164-168, 2015.
20. Bramlage CP, Tampe B, Koziolek M, Maatouk I, Bevanda J, Bramlage P, Ahrens K, Lange K, Schmid H, Cohen CD, *et al*: Bone morphogenetic protein (BMP)-7 expression is decreased in human hypertensive nephrosclerosis. BMC Nephrol 11: 31, 2010.
21. Klahr S and Morrissey J: Obstructive nephropathy and renal fibrosis: The role of bone morphogenic protein-7 and hepatocyte growth factor. Kidney Int Suppl 87: S105-S112, 2003.
22. Zeisberg M and Kalluri R: Reversal of experimental renal fibrosis by BMP7 provides insights into novel therapeutic strategies for chronic kidney disease. Pediatr Nephrol 23: 1395-1398, 2008.
23. Yu Z, Zai-Chun X, Wun-Lun H and Yun-Yun Z: BMP-7 attenuates TGF-β1-induced fibronectin secretion and apoptosis of NRK-52E cells by the suppression of miRNA-21. Oncol Res 23: 147-154, 2016.
24. Celic T, Spanjol J, Grskovic A, Markic D, Prebilic I, Fuckar Z and Bobinac D: Bone morphogenetic protein-7 reduces cold ischemic injury in rat kidney. Transplant Proc 43: 2505-2509, 2011.
25. Yanagita M, Okuda T, Endo S, Tanaka M, Takahashi K, Sugiyama F, Kunita S, Takahashi S, Fukatsu A, Yanagisawa M, *et al*: Uterine sensitization-associated gene-1 (USAG-1), a novel BMP antagonist expressed in the kidney, accelerates tubular injury. J Clin Invest 116: 70-79, 2006.
26. Yanagita M: Balance between bone morphogenetic proteins and their antagonists in kidney injury. Ther Apher Dial 11 (Suppl 1): S38-S43, 2007.
27. Collette NM, Yee CS, Hum NR, Murugesh DK, Christiansen BA, Xie L, Economides AN, Manilay JO, Robling AG and Loots GG: Sostdc1 deficiency accelerates fracture healing by promoting the expansion of periosteal mesenchymal stem cells. Bone 88: 20-30, 2016.
28. Murashima-Suginami A, Takahashi K, Sakata T, Tsukamoto H, Sugai M, Yanagita M, Shimizu A, Sakurai T, Slavkin HC and Bessho K: Enhanced BMP signaling results in supernumerary tooth formation in USAG-1 deficient mouse. Biochem Biophys Res Commun 369: 1012-1016, 2008.
29. Tanaka M, Asada M, Higashi AY, Nakamura J, Oguchi A, Tomita M, Yamada S, Asada N, Takase M, Okuda T, *et al*: Loss of the BMP antagonist USAG-1 ameliorates disease in a mouse model of the progressive hereditary kidney disease Alport syndrome. J Clin Invest 120: 768-777, 2010.
30. Tanaka M, Endo S, Okuda T, Economides AN, Valenzuela DM, Murphy AJ, Robertson E, Sakurai T, Fukatsu A, Yancopoulos GD, *et al*: Expression of BMP-7 and USAG-1 (a BMP antagonist) in kidney development and injury. Kidney Int 73: 181-191, 2008.
31. Yisireyili M, Hayashi M, Wu H, Uchida Y, Yamamoto K, Kikuchi R, Shoaib Hamrah M, Nakayama T, Wu Cheng X, Matsushita T, *et al*: Xanthine oxidase inhibition by febuxostat attenuates stress-induced hyperuricemia, glucose dysmetabolism, and prothrombotic state in mice. Sci Rep 7: 1266, 2017.
32. Day RO, Kamel B, Kannangara DR, Williams KM and Graham GG: Xanthine oxidoreductase and its inhibitors: Relevance for gout. Clin Sci (Lond) 130: 2167-2180, 2016.
33. Chinchilla SP, Urionaguena I and Perez-Ruiz F: Febuxostat for the chronic management of hyperuricemia in patients with gout. Expert Rev Clin Pharmacol 9: 665-673, 2016.
34. Sircar D, Chatterjee S, Waikhom R, Golay V, Raychaudhury A, Chatterjee S and Pandey R: Efficacy of febuxostat for slowing the GFR decline in patients with CKD and asymptomatic hyperuricemia: A 6-month, double-blind, randomized, placebo-controlled trial. Am J Kidney Dis 66: 945-950, 2015.
35. Fahmi AN, Shehatou GS, Shebl AM and Salem HA: Febuxostat exerts dose-dependent renoprotection in rats with cisplatin-induced acute renal injury. Naunyn Schmiedebergs Arch Pharmacol 389: 819-830, 2016.
36. Lee HJ, Jeong KH, Kim YG, Moon JY, Lee SH, Ihm CG, Sung JY and Lee TW: Febuxostat ameliorates diabetic renal injury in a streptozotocin-induced diabetic rat model. Am J Nephrol 40: 56-63, 2014.
37. Cao J, Li Y, Peng Y, Zhang Y, Li H, Li R and Xia A: Febuxostat prevents renal interstitial fibrosis by the activation of BMP-7 signaling and inhibition of USAG-1 expression in rats. Am J Nephrol 42: 369-378, 2015.
38. Manson SR, Niederhoff RA, Hruska KA and Austin PF: The BMP-7-Smad1/5/8 pathway promotes kidney repair after obstruction induced renal injury. J Urol 185 (6 Suppl): S2523-S2530, 2011.
39. Liu H, Xiong J, He T, Xiao T, Li Y, Yu Y, Huang Y, Xu X, Huang Y, Zhang J, *et al*: High uric acid-induced epithelial-mesenchymal transition of renal tubular epithelial cells via the TLR4/NF-κB signaling pathway. Am J Nephrol 46: 333-342, 2017.
40. Song S, Qiu D, Luo F, Wei J, Wu M, Wu H, Du C, Du Y, Ren Y, Chen N, *et al*: Knockdown of NLRP3 alleviates high glucose or TGFB1-induced EMT in human renal tubular cells. J Mol Endocrinol 61: 101-113, 2018.
41. Zeisberg M, Hanai J, Sugimoto H, Mammolo T, Charytan D, Strutz F and Kalluri R: BMP-7 counteracts TGF-beta1-induced epithelial-to-mesenchymal transition and reverses chronic renal injury. Nat Med 9: 964-968, 2003.

42. Sun J, Yin A, Zhao F, Zhang W, Lv J and Lv J: Protection of tubular epithelial cells during renal injury via post-transcriptional control of BMP7. Mol Cell Biochem 435: 141-148, 2017.
43. Zeisberg M, Shah AA and Kalluri R: Bone morphogenic protein-7 induces mesenchymal to epithelial transition in adult renal fibroblasts and facilitates regeneration of injured kidney. J Biol Chem 280: 8094-8100, 2005.
44. Massagué J and Chen YG: Controlling TGF-beta signaling. Genes Dev 14: 627-644, 2000.
45. Yanagita M, Oka M, Watabe T, Iguchi H, Niida A, Takahashi S, Akiyama T, Miyazono K, Yanagisawa M and Sakurai T: USAG-1: A bone morphogenetic protein antagonist abundantly expressed in the kidney. Biochem Biophys Res Commun 316: 490-500, 2004.
46. Omori H, Kawada N, Inoue K, Ueda Y, Yamamoto R, Matsui I, Kaimori J, Takabatake Y, Moriyama T, Isaka Y and Rakugi H: Use of xanthine oxidase inhibitor febuxostat inhibits renal interstitial inflammation and fibrosis in unilateral ureteral obstructive nephropathy. Clin Exp Nephrol 16: 549-556, 2012.
47. Hamasaki Y, Doi K, Okamoto K, Ijichi H, Seki G, Maeda-Mamiya R, Fujita T and Noiri E: 3-Hydroxy-3-methylglutaryl-coenzyme A reductase inhibitor simvastatin ameliorates renal fibrosis through HOXA13-USAG-1 pathway. Lab Invest 92: 1161-1170, 2012.
48. Peng L, He Q, Li X, Shuai L, Chen H, Li Y and Yi Z: HOXA13 exerts a beneficial effect in albumin-induced epithelial-mesenchymal transition via the glucocorticoid receptor signaling pathway in human renal tubular epithelial cells. Mol Med Rep 14: 271-276, 2016.
49. Lee JH, Kim JH, Kim JS, Chang JW, Kim SB, Park JS and Lee SK: AMP-activated protein kinase inhibits TGF-β-, angiotensin II-, aldosterone-, high glucose-, and albumin-induced epithelial-mesenchymal transition. Am J Physiol Renal Physiol 304: F686-F697, 2013.
50. Lee JY, Chang JW, Yang WS, Kim SB, Park SK, Park JS and Lee SK: Albumin-induced epithelial-mesenchymal transition and ER stress are regulated through a common ROS-c-Src kinase-mTOR pathway: Effect of imatinib mesylate. Am J Physiol Renal Physiol 300: F1214-F1222, 2011.
51. Wang S, Li Y, Song X, Wang X, Zhao C, Chen A and Yang P: Febuxostat pretreatment attenuates myocardial ischemia/reperfusion injury via mitochondrial apoptosis. J Transl Med 13: 209, 2015.
52. Tsuda H, Kawada N, Kaimori JY, Kitamura H, Moriyama T, Rakugi H, Takahara S and Isaka Y: Febuxostat suppressed renal ischemia-reperfusion injury via reduced oxidative stress. Biochem Biophys Res Commun 427: 266-272, 2012.
53. Nomura J, Busso N, Ives A, Matsui C, Tsujimoto S, Shirakura T, Tamura M, Kobayashi T, So A and Yamanaka Y: Xanthine oxidase inhibition by febuxostat attenuates experimental atherosclerosis in mice. Sci Rep 4: 4554, 2014.